

**EFFECT OF NONLINEAR ELECTRON-ELECTRON INTERACTION ON ELECTRON TUNNELING THROUGH AN ASYMMETRIC TWO-BARRIER RESONANCE TUNNEL STRUCTURE**

M.V. TKACH, JU.O. SETI, I.V. BOYKO

PACS 73.21.Fg, 73.90.+f,  
72.30.+q, 73.63.Hs  
©2012

Yu. Fed’kovych Chernivitsi National University  
(2, Kotsyubynskyi Str., Chernivtsi 58012, Ukraine; e-mail: ktf@chnu.edu.ua)

The quantum-mechanical theory for the transmission coefficient and the positive and negative conductivities of a monoenergetic electron flux through an open plane asymmetric two-barrier resonance tunnel structure, which can serve as an active element in quantum cascade lasers or quantum cascade detectors, has been developed in the framework of effective-mass and rectangular-potential models. The dependences of the transmission factor and the conductivity in such a structure on the electron energy and the frequency of an electromagnetic field are found. It is shown that the properties of the active conductivity can be used for the experimental evaluation of resonance energies and resonance widths of quasistationary electron states.

**1. Introduction**

The theory of electron transport through nano-sized two-barrier resonance tunnel structures (2BRTSs) – see Fig. 1 – is of importance, in particular, because those structures serve as the active elements of quantum cascade lasers and quantum cascade detectors operating in the range of electromagnetic waves belonging to the so-called atmosphere transparency windows. It is the properties of active conductivity in 2BRTSs that substantially govern such physical characteristics as the laser emission power, the excitation current, and so forth.

In the overwhelming majority of works [1–5], where the theory of physical processes in quantum cascade lasers and detectors was developed, the transport properties of electron fluxes through open resonance tunnel structures (RTSs) were studied. However, owing to mathematical difficulties met while solving the nonlinear differential equations, the electron-electron interac-

tion was not taken into account, as a rule. Note that, although the problems arising in the theory of nonlinear interaction between electrons in Bose systems and between quasiparticles in some other models were studied in a considerable number of works [6–11], the mathematical techniques developed there cannot be applied directly to the problem of transport of electrons, which interact with one another and with the electromagnetic field through open RTSs.

A similar problem was considered in works [12, 13]. However, to avoid substantial mathematical difficulties, a simplified RTS model, in which rectangular potential barriers were approximated by  $\delta$ -ones, was used there. The known shortcoming of this model consists in that the difference between the effective masses of electrons

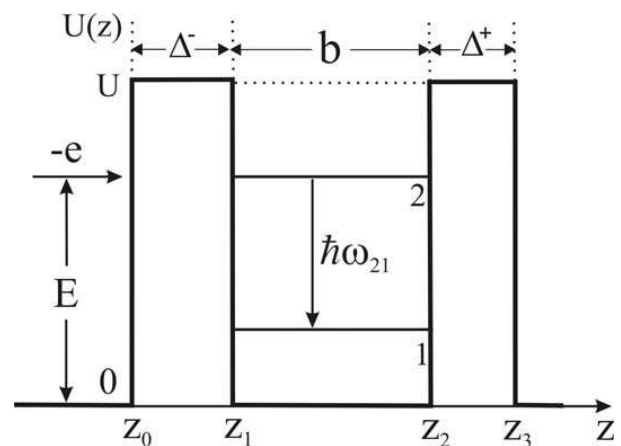


Fig. 1. Energy diagram of an electron in a 2BRTS

in wells and barriers, which does exist in real RTSs, turns out automatically ignored. This circumstance, together with the inadequacy of the  $\delta$ -approximation itself, gives rise to the overestimation of resonance energies for electron quasistationary states (QSSs) by tens percent and of the resonance widths by several tens of times. As a consequence, the electron lifetimes in all QSSs turn out underestimated by several tens of times in this simplified model, so that the conductivities become underestimated by several orders of magnitude.

This work aimed at developing the theory of transmission factor and active dynamic conductivity for a beam of interacting electrons in an open 2BRTS. The consideration is carried out with the use of the rectangular potential barrier model and assuming the different effective electron masses in wells and barriers of this nanosystem. The interaction with an electromagnetic field is taken into account in the weak-signal approximation.

## 2. Hamiltonian of the System. Transmission Factor and Active Conductivity of an Asymmetric 2BRTS

We consider an open plane asymmetric 2BRTS (Fig. 1) in a Cartesian coordinate system with the axis  $OZ$  directed normally to nanosystem planes. An insignificant difference between the lattice constants in the well and barrier layers of the nanostructure allows us to use the models of effective masses and rectangular potentials,

$$m(z) = m_0 \sum_{p=0}^2 (\theta(z - z_{2p-1}) - \theta(z - z_{2p})) + m_1 \sum_{p=0}^1 [\theta(z - z_{2p}) - \theta(z - z_{2p+1})], \quad (1)$$

$$U(z) = U \sum_{p=0}^1 [\theta(z - z_{2p}) - \theta(z - z_{2p+1})]. \quad (2)$$

Here,  $\theta(z)$  is the Heaviside function,  $z_{-1} = -\infty$ , and  $z_4 = \infty$ .

Let monoenergetic electrons with energy  $E$ , current density  $j_0^+ \sim \sqrt{E}$ , and concentration  $n_0$  move perpendicularly to the 2BRTS planes, for definiteness, from the left. Owing to this formulation of the problem, the motion of electrons can be considered as one-dimensional. Therefore, the complete Schrödinger equation for the wave function  $\Psi(E, z, t)$  looks like

$$i\hbar \frac{\partial \Psi(E, z, t)}{\partial t} = [H(E, z) + H(z, t)]\Psi(E, z, t), \quad (3)$$

where

$$H(E, z) = -\frac{\hbar^2}{2} \frac{\partial}{\partial z} \frac{1}{m(z)} \frac{\partial}{\partial z} + U(z) + v|\Psi(E, z)|^2 \quad (4)$$

is the Hamiltonian of a quasistationary problem (of the Gross–Pitaevskii type), which contains the nonlinear electron–electron interaction energy  $v|\Psi(E, z)|^2$  in the Hartree–Fock approximation, and the function  $\Psi(E, z)$  satisfies the stationary nonlinear Schrödinger equation

$$H(E, z)\Psi(E, z) = E\Psi(E, z). \quad (5)$$

The interaction Hamiltonian  $H(z, t)$  for an electron and a time-varying electromagnetic field with frequency  $\omega$  and a small strength  $\epsilon$  can be considered small, in the sense of perturbation theory. Consequently, this circumstance allowed us to write down the Hamiltonian in the following non-Coulomb gauge, which is convenient for analytical calculations:

$$H(z, t) = H(z)(e^{i\omega t} + e^{-i\omega t}), \quad (6)$$

where

$$H(z) = -e\epsilon\{z[\theta(z) - \theta(z - z_3)] + z_3\theta(z - z_3)\}.$$

Equation (3) has no exact solution. Therefore, taking into account that  $H(z, t)$  is small in the sense of perturbation theory, we can attempt to solve Eq. (3) in the so-called weak-signal approximation, when the wave function  $\Psi(E, z, t)$  is sought in the form

$$\Psi(E, z, t) = \Psi(E, z)e^{-i\omega_0 t} + \Psi_1(E, z, t) \quad (7)$$

where  $\omega_0 = E/\hbar$ , the function  $\Psi(E, z)$  satisfies Eq. (5), and the first-order correction to the wave function in the single-mode approximation is sought as

$$\Psi_1(E, z, t) = \Psi_{+1}(E, z)e^{-i(\omega_0 + \omega)t} + \Psi_{-1}(E, z)e^{-i(\omega_0 - \omega)t}. \quad (8)$$

Preserving the quantities down to the first order of smallness in Eq. (3) and taking Eqs. (7) and (8) into account, we obtain the following system of two inhomogeneous equations for the functions  $\Psi_{\pm 1}(E, z)$ :

$$[H(E, z) - \hbar(\omega_0 \pm \omega)]\Psi_{\pm 1}(E, z) + H(z)\Psi(E, z) = 0. \quad (9)$$

To solve this system, it is necessary to know the analytical expression for the function  $\Psi(E, z)$ , which is a solution of the nonlinear Schrödinger equation (5). Since the 2BRTS is open, Eq. (5) has to be solved with regard for the continuity conditions for the wave function and

the flux density across all the boundaries and interfaces ( $\eta \rightarrow +0$ ) of the system,

$$\Psi^{(p)}(E, z_p - \eta) = \Psi^{(p+1)}(E, z_p + \eta); (p = 0 \div 3),$$

$$\frac{\partial \Psi^{(p)}(E, z)}{m(z)\partial z} \Big|_{z=z_p-\eta} = \frac{\partial \Psi^{(p+1)}(E, z)}{m(z)\partial z} \Big|_{z=z_p+\eta}, \quad (10)$$

and the normalization condition

$$\int_{-\infty}^{\infty} \Psi^*(k', z)\Psi(k, z) = \delta(k - k'). \quad (k = \hbar^{-1}\sqrt{2m_0E}). \quad (11)$$

The wave function  $\Psi(E, z)$  in the nonlinear Schrödinger equation (5) can be found using two methods: (i) the Monte-Carlo numerical technique and (ii) the iteration technique. The Monte-Carlo technique was used to calculate wave functions for specific systems with a relatively low nonlinearity, for which the results obtained almost precisely coincided with those obtained by the iteration technique. An advantage of the latter consists in that it allows the wave functions for the nonlinear Schrödinger equation (5) to be obtained quickly and with a necessary accuracy within the reasonable computation time interval of a personal computer, even if the energy of a nonlinear interaction between electrons is high.

The procedure of solving the nonlinear Schrödinger equation (5) by the iteration technique is as follows. First, we solve the linear Schrödinger equation (without interaction)

$$H_0\Psi_0(E, z) = E\Psi_0(E, z). \quad (12)$$

Its exact solution is known [14],

$$\begin{aligned} \Psi_0(E, z) = & (A_0(E)e^{ik_0z} + B_0(E)e^{-ik_0z})\theta(-z) + \\ & + \sum_{p=1}^3 A_p(E)e^{ik_pz} + B_p(E)e^{-ik_pz} \left[ \theta(z - z_{p-1}) - \right. \\ & \left. - \theta(z - z_p) \right] + A_4(E)e^{ik_0z}(z - z_3), \end{aligned} \quad (13)$$

where the coefficients  $A_p(E)$ ,  $B_p(E)$ ,  $B_0(E)$ , and  $A_4(E)$  are determined unambiguously in terms of the coefficient  $A_0(E)$ . The latter, in turn, is connected with the density  $j_0^+$  of the initial electron flux that arrives at the 2BRTS

by the relation  $j_0^+ = en_0\sqrt{2Em_0^{-1}}|A_0(E)|^2$ , where  $n_0$  is the concentration of electrons in this flux, and  $e$  the electron charge.

The quantities  $k_p$  ( $p = 0 \div 4$ ) are determined by the dynamic characteristics of an electron,

$$k_0 = k_2 = k_4 = k = \hbar^{-1}\sqrt{2m_0E};$$

$$k_1 = k_3 = \hbar^{-1}\sqrt{2m_1(E - U)} \quad (14)$$

whereas the quantities  $z_p$  ( $p = 0 \div 3$ ) by the geometrical dimensions of elements in the 2BRTS,

$$z_0 = 0; \quad z_1 = \Delta^-; \quad z_2 = b + \Delta^-; \quad z_3 = b + \Delta^- + \Delta^+. \quad (15)$$

The function  $\Psi_0(E, z)$  found in form (13) does not allow the Schrödinger equation (5) to be solved directly. However, the now known function  $|\Psi_0(E, z)|^2$  can always be represented in the form of a sum of  $N$  piecewise continuous functions,

$$\begin{aligned} |\Psi_0(E, z)|^2 = & \lim_{N \rightarrow \infty} \sum_{p=0}^N |\Psi_0(E, z_{2p})|^2 \times \\ & \times [\theta(z - z_{2p-1}) - \theta(z - z_{2p+1})], \end{aligned} \quad (16)$$

where

$$z_p = \frac{p}{2N}b; \quad z_{-1} = z_0 = 0; \quad z_{2N} = z_{2N+1} = b + \Delta^- + \Delta^+.$$

The examples of the dependence of this function on  $E$  and  $z$  are depicted in Fig. 2, a.

Hence, if the value of  $N$  is large enough,  $N \gg 1$ , the continuous function  $|\Psi_0(E, z)|^2$  can always be approximated with a required accuracy by a piecewise continuous function,  $|\tilde{\Psi}_0(E, z)|^2 \approx |\Psi_{0N}(E, z)|^2$ . As a result, the nonlinear potential  $v|\Psi_0(E, z)|^2$  in Eq. (5) transforms into a piecewise linear potential  $v|\tilde{\Psi}_0(E, z)|^2$ . The latter provides the solution for the approximated nonlinear Schrödinger equation (5), if the continuity equations of type (10) are obeyed at each point  $z_{2p-1}$ , so that the nonlinear function  $\Psi(E, z)$  can be determined in the first approximation,  $\Psi_I(E, z)$ .

Knowing the function  $\Psi_I(E, z)$ , we calculate  $|\Psi_I(E, z)|^2$  and represent it as a piecewise continuous function (provided that  $N \gg 1$ )

$$|\tilde{\Psi}_I(E, z)|^2 = \lim_{N \rightarrow \infty} \sum_{p=0}^N |\Psi_I(E, z_{2p})|^2 \times$$

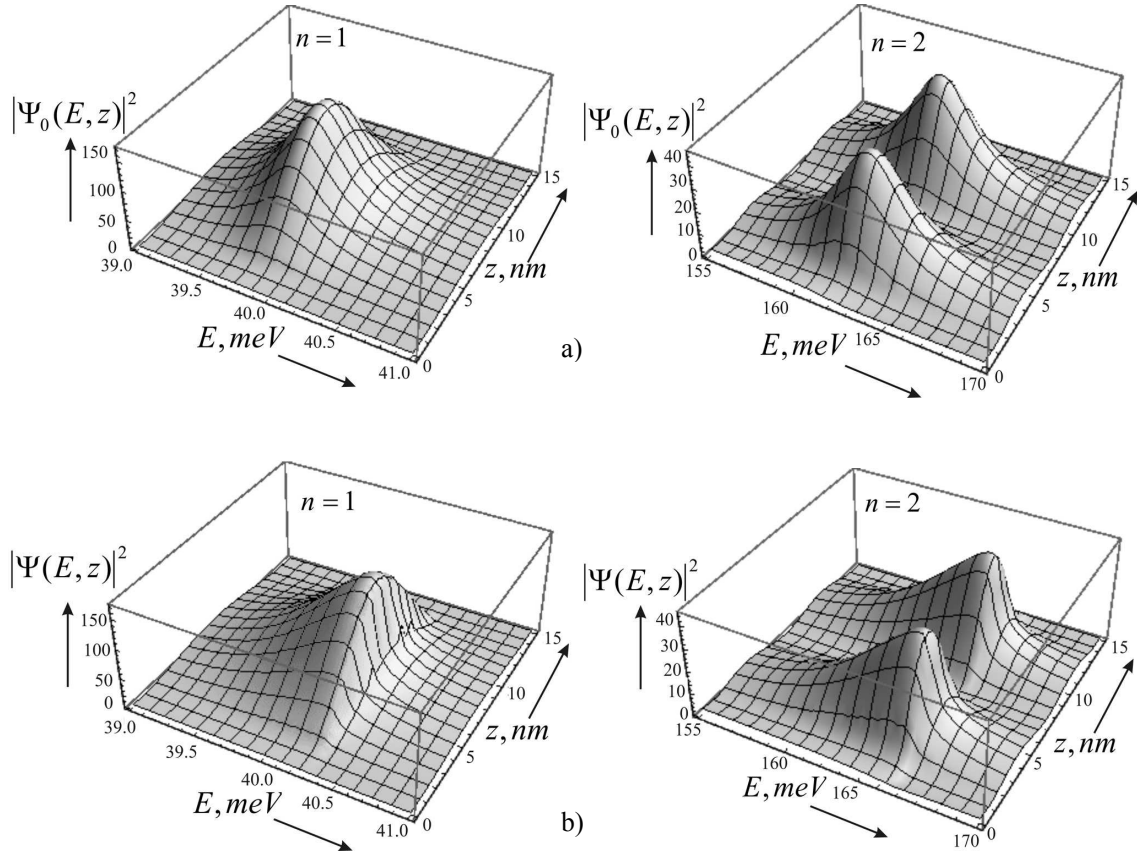


Fig. 2. Dependences  $|\Psi(E, z)|^2$  for two first ( $n = 1, 2$ ) QSSs in a 2BRTSs with the geometrical parameters  $\Delta^- = \Delta^+ = 2.1$  nm and  $b = 10.8$  nm calculated for  $v = 0$  (panels a,  $n = 1, 2$ ),  $10^{-3}$  (panel b,  $n = 1$ ), and  $0.01$  meV (panel b,  $n = 2$ )

$$\times [\theta(z - z_{2p-1}) - \theta(z - z_{2p+1})]. \quad (17)$$

Being substituted into the Schrödinger equation (5), together with boundary conditions of type (10) at each point  $z_{2p-1}$ , the function  $|\tilde{\Psi}_I(E, z)|^2$  linearizes the potential in the  $z$ -intervals, which allows the Schrödinger equation to be solved again and the wave function  $\Psi(E, z)$  to be determined in a second iteration (approximation),  $\Psi_{II}(E, z)$ .

Using this iteration way, we determine the wave function  $\Psi(E, z)$  as a solution of the nonlinear Schrödinger equation (5) in an arbitrary  $S$ -th iteration cycle,

$$\Psi(E, z) = \Psi_S(E, z). \quad (18)$$

The number of iteration cycles,  $S$ , which are to be executed while iteratively calculating  $\Psi(E, z)$ , is associated with a required accuracy, the latter being controlled by the evident condition

$$\zeta = \max_{E, z} \left\{ \frac{|\Psi_S(E, z)|^2 - |\Psi_{S-1}(E, z)|^2}{|\Psi_S(E, z)|^2} \right\} \ll 1. \quad (19)$$

It is clear that, for a given accuracy of  $\Psi(E, z)$ -calculations  $\zeta$ , the number of iterations depends on the magnitude of electron-electron interaction potential  $v$ : the larger the magnitude, the larger the number of iteration cycles  $S$  is required.

The examples of the dependence of  $|\Psi(E, z)|^2$  on  $E$  and  $z$  obtained for the studied system in a vicinity of the energies of two first electron QSSs at various values of potential  $v$  are exhibited in Fig. 2, b. Note that the results of calculations shown in Fig. 2, which were obtained by using both calculation techniques, are practically identical and, therefore, no difference between them is observed. The found wave function (18), according to the quantum-mechanical theory [15], allows the transmission factor for a flux of interacting electrons through a 2BRTS to be calculated as

$$D(E) = |A_0(E)|^{-2} \text{Im} \left\{ \Psi(E, z) \frac{\partial \Psi(E, z)}{k \partial z} \right\}_{z=z_3+\eta}. \quad (20)$$

It is known [14, 15] that the transmission factor  $D(E)$  is needed to calculate such spectral parameters of elec-

tron QSSs, as the resonance energies and widths. The positions of maxima in the dependence  $D(E)$  determine the resonance energies,  $E_n$ , and their half-height widths do the resonance widths,  $\Gamma_n$ , of QSSs. As an example, the  $D(E)$ -properties of a 2BRTS that is often studied experimentally [16–19] are analyzed in the next section.

The found wave function  $\Psi(E, z)$  allows the solutions of the inhomogeneous equations (9) to be obtained in the form

$$\Psi_{\pm 1}(E, z) = \Psi_{\pm}(E, z) + \Phi_{\pm}(E, z), \quad (21)$$

where  $\Psi_{\pm}(E, z)$  are the solutions of homogeneous Eq.s. (9), and  $\Phi_{\pm}(E, z)$  are the exact partial solutions of their inhomogeneous counterparts. The solutions of the homogeneous equations are sought in the form

$$\begin{aligned} \Psi_{\pm}(E, z) = & \\ = \sum_{p=0}^4 & \left[ B_{\pm}^{(p)}(E) e^{-ik_{\pm}^{(p)} z} + A_{\pm}^{(p)}(E) e^{ik_{\pm}^{(p)} z} \right] \times \\ \times & [\theta(z - z_{p-1}) - \theta(z - z_p)], \quad A_{\pm}^{(0)}(E) = B_{\pm}^{(4)}(E) = 0, \end{aligned} \quad (22)$$

where

$$\begin{aligned} k_{\pm}^{(0)} = k_{\pm}^{(2)} = k_{\pm}^{(4)} &= \sqrt{2m_0(E \pm \hbar\omega)/\hbar^2}, \\ k_{\pm}^{(1)} = k_{\pm}^{(3)} &= \sqrt{2m_1((E - U) \pm \hbar\omega)/\hbar^2}. \end{aligned} \quad (23)$$

The partial solutions of system (9) are known,

$$\begin{aligned} \Phi_{\pm}(E, z) = & \\ = \sum_{p=1}^3 & \left[ \mp \frac{e\epsilon z}{\hbar\omega} \Psi_0^{(p)}(E, z) + \frac{e\epsilon}{m(z)\omega^2} \frac{d\Psi_0^{(p)}(E, z)}{dz} \right] \times \\ \times & [\theta(z - z_{p-1}) - \theta(z - z_p)] \mp \frac{e\epsilon z_3}{\hbar\omega} \Psi_0^{(4)}(E, z_3) \theta(z - z_3). \end{aligned} \quad (24)$$

The continuity conditions for the wave functions (21) and the corresponding fluxes at all boundaries and interfaces of the nanosystem give rise to a system of eight inhomogeneous equations, which is used to determine eight coefficients  $B_{\pm}^{(0)}(E)$ ,  $A_{\pm}^{(4)}(E)$ ,  $B_{\pm}^{(p)}(E)$ , and  $A_{\pm}^{(p)}(E)$  ( $p = 1 \div 3$ ). Hence, we have the unambiguously determined functions  $\Psi_{\pm}(E, z)$ , the first-order correction  $\Psi_1(E, z, t)$ , and the total wave function  $\Psi(E, z, t)$ . According to quantum-mechanical theory, the total wave

function of electrons interacting with a periodic-in-time electromagnetic field determines the density of an electron flux through a nanostructure by the formula

$$\begin{aligned} j(E, z, t) = & \frac{ie\hbar n_0}{2m(z)} \times \\ \times & \left( \Psi(E, z, t) \frac{\partial}{\partial z} \Psi^*(E, z, t) - \Psi^*(E, z, t) \frac{\partial}{\partial z} \Psi(E, z, t) \right). \end{aligned} \quad (25)$$

Below, in view of the smallness of 2BRTS dimensions in comparison with the electromagnetic wave length, in the quasiclassical approximation and in the case of quantum transitions accompanied by the energy emission (absorption), we calculate the reduced current, which determines the absolute value of negative (positive) active dynamic conductivity in the nanosystem,

$$\sigma(E, \omega) = \sigma^+(E, \omega) + \sigma^-(E, \omega), \quad (26)$$

where

$$\begin{aligned} \sigma^+(E, \omega) &= \frac{\hbar^2 \omega n_0}{2m_0 z_3 \epsilon^2} \left( k_+^{(0)} |B_+^{(0)}(E)|^2 - k_-^{(0)} |B_-^{(0)}(E)|^2 \right), \\ \sigma^-(E, \omega) &= \frac{\hbar^2 \omega n_0}{2m_0 z_3 \epsilon^2} \left( k_+^{(4)} |A_+^{(4)}(E)|^2 - k_-^{(4)} |A_-^{(4)}(E)|^2 \right). \end{aligned}$$

Here,  $\sigma^+(E, \omega)$  and  $\sigma^-(E, \omega)$  are the partial components of the conductivity associated with fluxes of electrons with energy  $E$  that interact with an electromagnetic field with frequency  $\omega$  and quit the system in the direction that, respectively, coincides with or is opposed to that of the initial electron flux incident onto the 2BRTS.

### 3. Influence of Nonlinear Electron-Electron Interaction on the Transmittance and the Dynamic Conductivity of 2BRTS

The influence of the nonlinear electron-electron interaction on the transmission coefficient and the dynamic conductivity of an open 2BRTS will be studied on the basis of a plane nanostructure composed of alternating  $\text{In}_{0.53}\text{Ga}_{0.47}\text{As}$ -wells and  $\text{In}_{0.52}\text{Al}_{0.48}\text{As}$ -barriers with the parameters  $m_0 = 0.046m_e$ ,  $m_1 = 0.081m_e$ ,  $U = 516$  meV, and  $n_0 = 10^{16} \text{ cm}^{-3}$ . In what follows, we assume that  $A_0 = 1$ .

In order to understand why the transmission factor  $D(E, v)$  and the active conductivity  $\sigma(E, \omega, v)$  change, by depending on the quantity  $v$ , we exhibit, in Fig. 2, *b*,

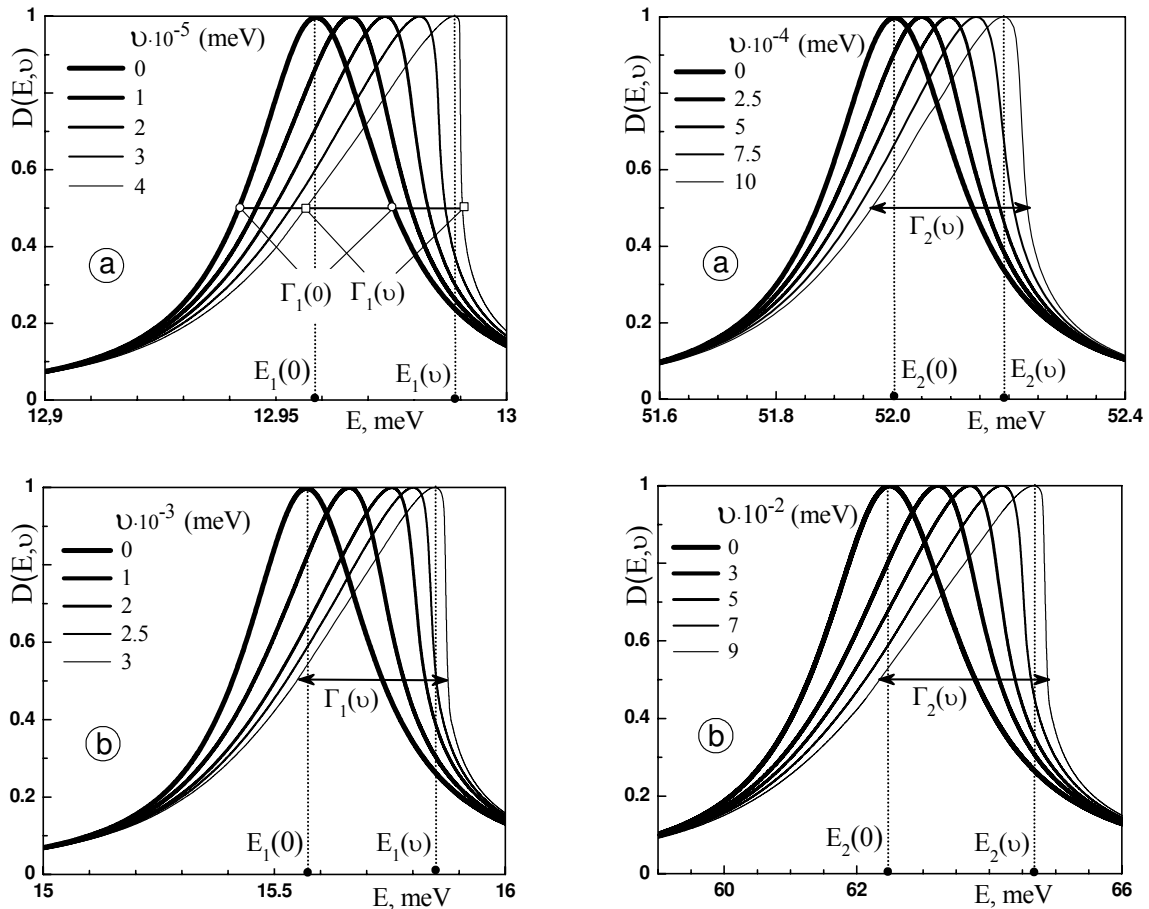


Fig. 3. Dependences of the transmission factor on the electron energy in vicinities of two first QSSs at different values of electron-electron interaction energy  $v$  for a 2BRTS with the parameters  $\Delta^+ = \Delta^- = 2.1$  nm and  $b = 21.6$  nm calculated in the (a) rectangular potential and (b)  $\delta$ -barrier models

the examples of the dependence of  $|\Psi(E, z)|^2$  on the energy  $E$  and the coordinate  $z$  in a vicinity of the energies of two first QSSs calculated for different magnitudes of electron-electron interaction energy,  $v$ . From this figure, one can see that, irrespective of  $v$ -magnitude, the function  $|\Psi(E, z)|^2$  at  $E = \text{const}$  has  $n$  maxima in a vicinity of the  $n$ -th QSS, similarly to what takes place in the case of a closed nanosystem. If the coordinate value  $z$  is fixed, the quantity  $|\Psi(E, z = \text{const})|^2$  considered as a function of the energy deviates more and more from the Lorentzian shape, being so deformed that its high-energy wing falls down more abruptly, whereas the low-energy one gradually rises up and becomes flatter.

The revealed properties of  $|\Psi(E, z)|^2$  are responsible for the corresponding evolution of the shape of the transmission coefficient,  $D$ , depending on the energy  $E$  in vicinities of the first and second QSSs at different values of electron-electron interaction potential  $v$  (see Fig. 3,a).

For comparison, in Fig. 3,b, we also show the evolution of  $D(E, v)$  with the varying  $v$  calculated for the same 2BRTS in the framework of the  $\delta$ -barrier model. Figure 3 demonstrates that the  $\delta$ -barrier model overestimates the resonance energies of electron QSSs by tens percent and the resonance widths by several tens of times in comparison with the model of rectangular potentials. Therefore, the selection of a realistic model for the electron-electron interaction results in a substantial deformation of the transmission factor dependence, even if the magnitude of electron-electron interaction is two orders of magnitude weaker than that given by the  $\delta$ -barrier model. From Fig. 3, one can also see that the evolution of  $D(E, v)$  at  $v = 0$  is qualitatively identical in both models. The transmission coefficient  $D(E, v)$  has the Lorentzian shape with the maximum value  $D(E_n, v) = 1$  at every resonance energy  $E_n$  and the half-height width  $\Gamma_n(v)$  for every ( $n$ -th) QSS. As the electron-electron

interaction energy grows, the shape of the coefficient  $D(E, v)$  in vicinities of the renormalized resonance energies  $E_n$  becomes firstly quasi-Lorentzian for every QSS. With a further increase of  $v$ , the function  $D(E, v)$  becomes more and more deformed, so that its low-energy wing slowly rises in the maximum vicinity to acquire a quasilinear dependence on  $E$ , whereas the high-energy wing drastically—almost steeply—falls down. Hence, if the  $v$ -value is large enough (for a larger QSS ordinary number, this value should also be larger), the shape of  $D(E, v)$  differs drastically from the Lorentzian in vicinities of the resonance energies renormalized by the interaction,  $E_n$ , becoming wedge-like (see Fig. 3). Therefore, we need to generalize the concepts of resonance energy,  $E_n$ , and width,  $\Gamma_n$ , of a symmetric Lorentzian curve, so that it could be extended to include the wedge-shaped form of the  $D(E, v)$ -dependence.

A way to implement such a generalization is illustrated in Fig. 4. Really, the generalization of the resonance energies  $E_n(v)$  is evident. At the same time, it is expedient to introduce the generalized resonance width  $\Gamma_n(v)$  of the  $n$ -th QSS as a sum of low-,  $\gamma_{nd}(v)$ , and high-energy,  $\gamma_{nh}(v)$ , half-widths, because, since  $\gamma_{nd}(v \rightarrow 0) = \gamma_{nh}(v \rightarrow 0) = \Gamma_n(0)/2$ , the introduced quantities provide the correct passage to the limit  $\Gamma_n(v \rightarrow 0) = \Gamma_n$ . The expediency and the convenience of using the generalized resonance energies and widths as generalized spectral parameters of the coefficient  $D(E, v)$  are illustrated in Fig. 4. The figure demonstrates the dependences of the generalized resonance energy  $E_n$  and the generalized resonance width  $\Gamma_n$ —the latter as the distance between the curves  $E_n(v) + \gamma_{nh}(v)$  and  $E_n(v) - \gamma_{nd}(v)$ —on the magnitude of electron-electron interaction  $v$ .

Asymmetric structures are often dealt with in practice. Therefore, an important task is to study the behavior of generalized resonance widths and energies with respect to the electron-electron interaction energy in 2BRTSs with various thicknesses of the input,  $\Delta^-$ , and output,  $\Delta^+$ , barriers. In order to generalize the results of our research qualitatively and quantitatively, let us consider an asymmetric 2BRTS, the thicknesses of both barriers in which satisfying the condition  $\Delta = \Delta^+ + \Delta^- = \text{const}$ . In Fig. 4, the dependences of the generalized resonance energies and the widths of two first QSSs on the electron-electron interaction energy  $v$  calculated at various  $\Delta^+$ - and  $\Delta^-$ -values are depicted. The plots completely explain the quasi-Lorentzian shape of the dependence of the transmission factor  $D(E, v)$  on the energy  $E$ .

Figure 4 demonstrates that, when the thickness of the input barrier  $\Delta^-$  becomes narrower and the thickness

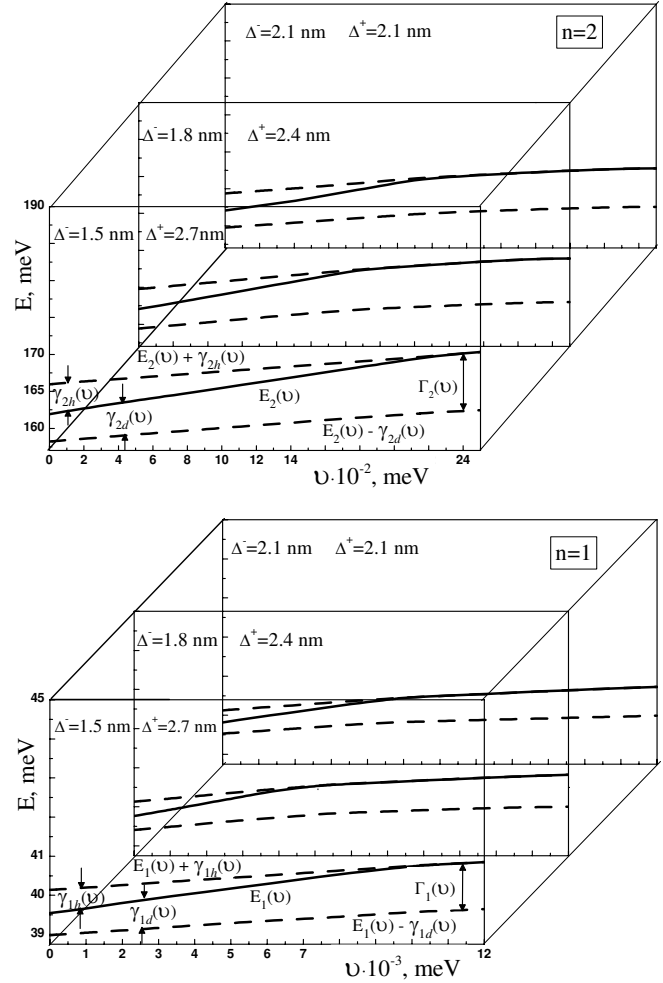


Fig. 4. Dependences of the resonance energies and widths for first two electron QSSs on the electron-electron interaction energy  $v$  in a 2BRTS with the geometrical parameters  $b = 10.8$  nm and  $\Delta^- + \Delta^+ = 4.2$  nm

of the output barrier  $\Delta^+$  wider by the same amount, the resonance energy and width grow. If the  $v$ -value is low, the generalized resonance widths  $\gamma_{nd}(v)$  and  $\gamma_{nh}(v)$  are, at first, almost identical ( $\gamma_{nd}(v) \approx \gamma_{nh}(v)$ ) irrespective of the barrier-to-width ratio. When the energy of the electron-electron interaction increases,  $\gamma_{nh}(v)$  decreases, and  $\gamma_{nd}(v)$  increases. At some critical  $v_{cr}$ , we obtain  $\Gamma_n(v_{cr}) = \gamma_{nd}(v_{cr})$  and  $\gamma_{nh}(v_{cr}) = 0$ . Note also that, when the electron-electron interaction energy varies, the generalized resonance width practically remains unchanged,  $\Gamma_n(v) = \gamma_{nd}(v) + \gamma_{nh}(v) = \text{const}$ .

Figure 4 also demonstrates that every two-barrier nanostructure with a specific  $\Delta^-/\Delta^+$ -ratio is characterized by a corresponding critical value  $v_{cr}$ , which grows, if the difference between the thicknesses of both bar-

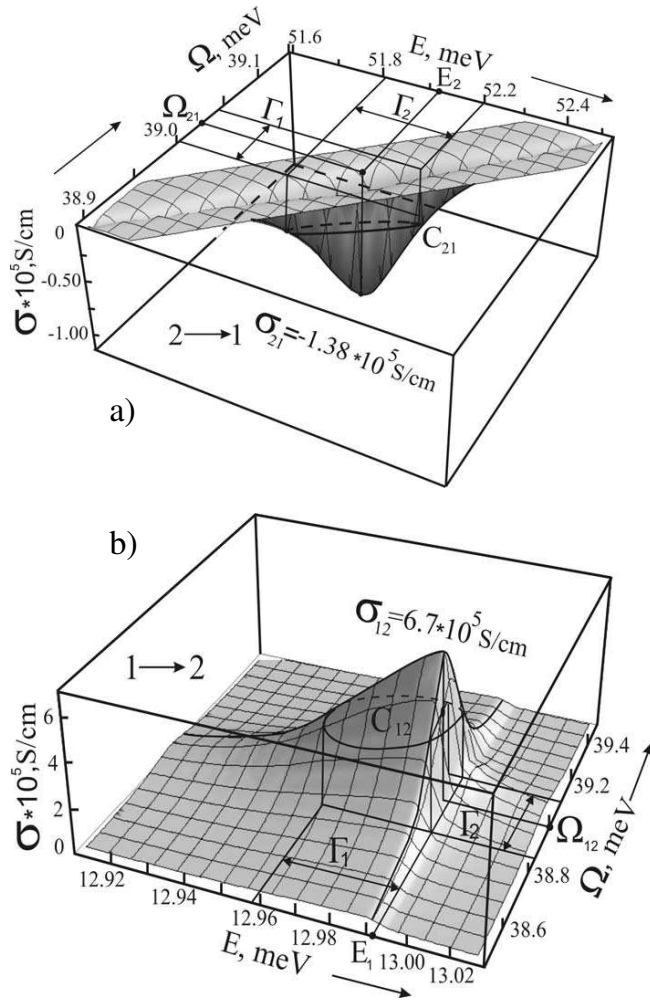


Fig. 5. Dependences of the dynamic conductivity  $\sigma$  in a 2BRTS on the electron energy  $E$  and the electromagnetic field energy  $\Omega = \hbar\omega$  calculated for  $v = 5 \times 10^{-4}$  meV and (a) a laser quantum transition and (b) a detector quantum transition

riers increases. Whence it follows that the electron-electron interaction in symmetric 2BRTSs manifests itself at lower values with respect to those in structures with different thicknesses of input and output barriers. Since the active dynamic conductivity  $\sigma$  depends on the geometrical parameters of RTS (through the spectral parameters of quasistationary states of an electron), it also considerably depends on the energy  $E$  of incident electrons and the energy  $\Omega = \hbar\omega$  of an electromagnetic field that interacts with them.

The characteristic dependences of the negative and positive conductivities  $\sigma$  on  $E$  and  $\Omega$ , which were calculated for a 2BRTS with the geometrical parameters  $b = 21.6$  nm and  $\Delta^- = \Delta^+ = 2.4$  nm are shown in

Fig. 5. The negative conductivity  $\sigma(E, \Omega)$  at the laser transition ( $2 \rightarrow 1$ ) was calculated in the energy interval containing the energy  $E_2$  of the second electron resonance, to which the electron flux is directed, and in the range of the electromagnetic field energy containing the energy  $\Omega = E_2 - E_1$  of the electromagnetic wave emitted as a result of quantum-mechanical transition from the quasistationary state with the energy  $E_2$  into the state with the energy  $E_1$ . For the detector transition ( $1 \rightarrow 2$ ), the calculation of  $\sigma(E, \Omega)$  was carried out in the energy range containing the energy  $E_1$  of the first electron resonance, to which the electron flux is directed, and in the range of the electromagnetic field energy containing the energy  $\Omega = |E_1 - E_2|$  of the electromagnetic wave absorbed as a result of the quantum-mechanical transition from the quasistationary state with the energy  $E_1$  into the state with the energy  $E_2$ . The negative active conductivity arises in the case of a laser transition and the positive one in the case of a detector transition.

From Fig. 6, one can see the major properties of the dynamic conductivity  $\sigma(E, \Omega)$  as functions of  $E$  and  $\Omega$ , which are associated with quantum-mechanical transitions between electron QSSs as a result of the emission or absorption of the electromagnetic field energy. In the  $(E, \Omega)$ -plane, the function  $\sigma(E, \Omega)$  has a minimum  $\sigma_{21} = \sigma(E_2, \Omega_{21} = E_2 - E_1)$  in the case of a laser transition and a maximum  $\sigma_{12} = \sigma(E_1, \Omega_{12} = |E_1 - E_2|)$  in the case of a detector one.

Cross-sections of the surface  $\sigma(E, \Omega)$  by the vertical planes passing through  $\sigma_{21}$  and  $\sigma_{12}$  are curves with a quasi-Lorentzian shape at  $v = 0$  and with a wedge-like one at large  $v$ 's (Fig. 6). From Fig. 6, one can also see that the extrema of the functions  $\sigma(E, \Omega = \text{const})$  for a laser (panel a) or detector (panel b) transition become shifted toward higher energies as the interaction,  $v$ , increases. On the electron energy scale,  $E$ , those extrema correspond to the resonance energies of the second,  $E_2$ , and first,  $E_1$ , QSSs, respectively. The increase of the interaction,  $v$ , irrespective of the sign of the dynamic conductivity  $\sigma$ , deforms the shape of its dependence on  $E$  from quasi-Lorentzian to wedge-like, so that the low-energy wing depends on  $E$  linearly, whereas the high-energy one falls down abruptly by magnitude.

Cross-sections of the surface  $\sigma(E, \Omega)$  by a horizontal plane at the heights  $\sigma_{12}/2$  and  $\sigma_{21}/2$  are closed contours ( $C_{12}$  and  $C_{21}$ , respectively), the projections of which onto the corresponding axes  $(E, \Omega)$ , as is seen from Fig. 7, practically coincide with the spectral parameters of those working quasistationary

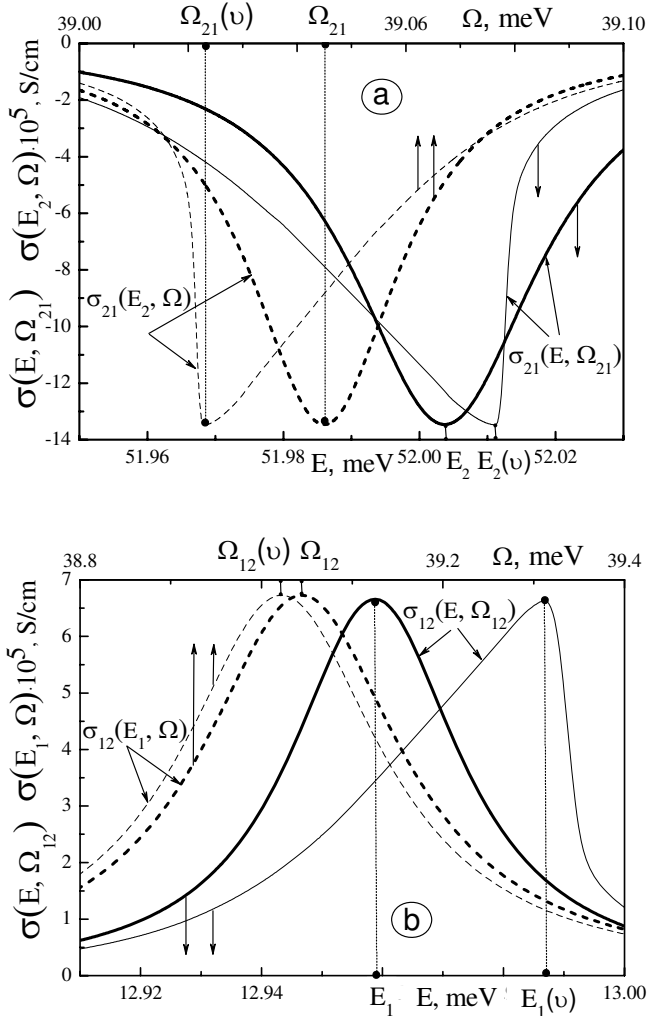


Fig. 6. Dependences of the (a) negative and (b) positive dynamic conductivities  $\sigma$  on the energy  $E$  (at  $\Omega = \text{const}$ ) and  $\Omega$  (at  $E = \text{const}$ ) at  $v = 0$  (bold solid and dashed curves) and  $5 \times 10^{-4}$  meV (thin solid and dashed curves)

states, between which the quantum transition responsible for the peaks in  $\sigma(E, \Omega)$  in the cases of the laser (panel a) and detector (panel b) transitions takes place.

In Fig. 8, some dependences of the absolute value of negative conductivity,  $|\sigma(E, \Omega, v)|$ , on the electromagnetic field energy  $\Omega$  calculated for a 2BRTS with the geometrical parameters  $\Delta^+ = \Delta^- = 2.4$  nm and  $b = 21.6$  nm are shown. We presented the results obtained for  $v = 0$  and  $5 \times 10^{-5}$  meV and several values of electron energy  $E$  within the range  $E_2 - \Gamma_2/2 \leq E \leq E_2 + \Gamma_2/2$ . The figure also exhibits the dependences of the transmission factor on the electron energy in a vicinity of the generalized resonance energy of the second (in the main

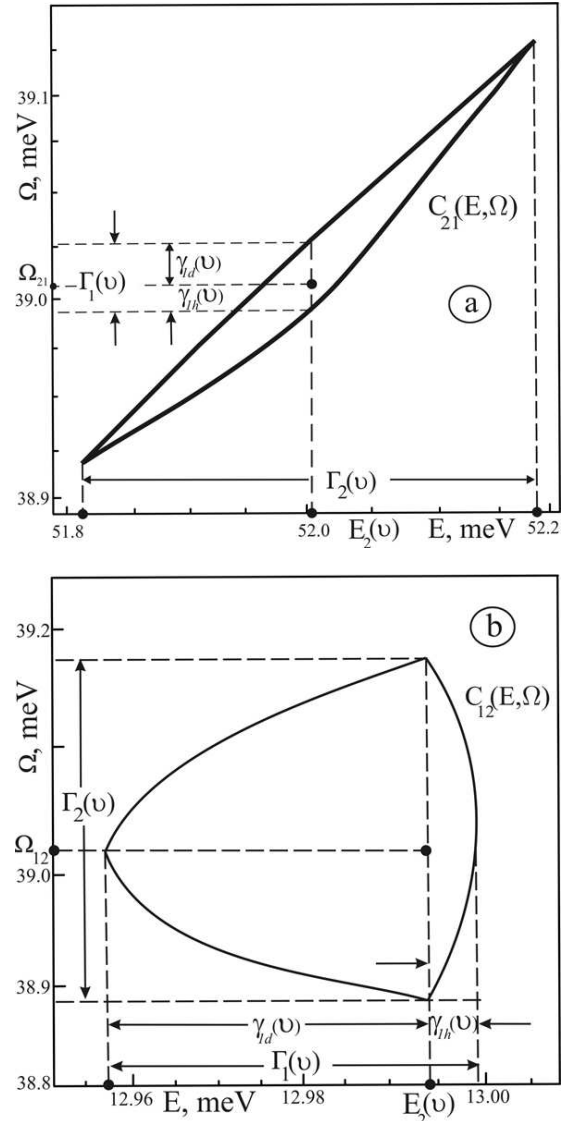


Fig. 7. Contours  $C(E, \Omega)$  for (a) negative and (b) positive conductivities. Relations of their projections onto the  $E$ - and  $\Omega$ -axes with the spectral parameters—the resonance energy and width—of the first and second QSSs at  $v = 5 \times 10^{-4}$  meV

panel) and first (in the inset) QSSs on the same energy  $E$  scale, as the  $\Omega$  one, and for the same  $v$ -values. It is evident that, in a vicinity of the generalized resonance energy of the second QSS, the transmission coefficient  $D(E, v)$  practically coincides (the difference is practically inobservable in the figure) with the dependence on  $\Omega$  of the normalized envelope function (with respect to the energy  $E$ )

$$\tilde{\sigma}(E, \Omega, v) =$$

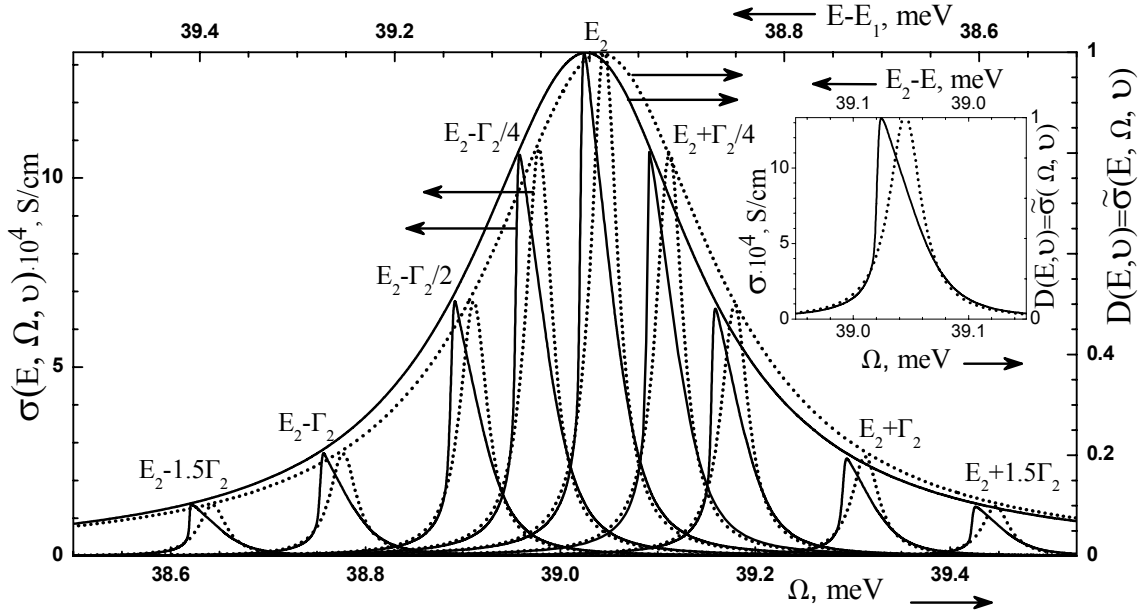


Fig. 8. Active conductivity  $\sigma$  (the left axis) as a function of the electromagnetic field energy  $\Omega$  (the bottom axis) at various electron energies  $E$ . Transmission factor  $D$  (the right axis) as a function of the energy  $E$  (the upper axis). Dashed curves correspond to  $\nu = 0$ , and solid ones to  $\nu = 5 \times 10^{-4}$  meV

$$= \sigma(E, \Omega, \nu) / \sigma(E_2(\nu), E_2(\nu) - E_1(\nu), \nu) \quad (27)$$

irrespective of the  $\nu$ -value. At the same time, in a vicinity of the generalized resonance energy of the first QSS, it coincides with the normalized active conductivity

$$\tilde{\sigma}(E_2, \Omega, \nu) = \sigma(E_2, \Omega, \nu) / \sigma(E_2(\nu), \Omega, \nu). \quad (28)$$

Figure 8 also demonstrates that the electron-electron interaction practically does not affect the maximal value of conductivity  $\sigma(E, \Omega)$ , but shifts—weakly and proportionally to the interaction energy  $\nu \max |\Psi(E, z)|^2$ —the function  $\sigma(E, \Omega)$  toward lower frequencies and deforms its shape from Lorentzian to wedge-like.

#### 4. Conclusions

Taking the electron-electron interaction into account, a quantum-mechanical theory of electron conductivity in an open 2BRTS, considered as the active element in a quantum cascade laser or a quantum cascade detector, has been developed. The electron-electron interaction is found to weakly affect the magnitude of dynamic conductivity and, irrespective of its sign, shifts the position of its extremum toward higher electron energies and lower energies of the electromagnetic field. If the electron-electron interaction is considerable, the dynamic conductivity  $\sigma$ , as a function of the electron energy, becomes

wedge-shaped. At the same time, in absorption processes, it remains quasi-Lorentzian as a function of the electromagnetic field strength. The scanning of the active dynamic conductivity of a 2BRTS using a monoenergetic electron beam with energy  $E$  allows the dependence of  $\sigma$  on  $E$  and  $\Omega$  to be determined experimentally, which enables important spectral parameters – the generalized resonance energies and widths of electron QSSs – to be estimated.

1. V.F. Elesin, JETP **101**, 44 (2005).
2. A.B. Pashkovskii, JETP Lett. **89**, 34 (2009).
3. Ju. Seti, M. Tkach, and O. Voitsekhivska, Cond. Mat. Phys. **14**, 13701 (2011).
4. A.F. Klinskikh, D.A. Chechin, and A.V. Dolgikh, J. Phys. B **41**, 161001 (2008).
5. Q.K. Yang and A.Z. Li, J. Phys. Cond. Matter **12**, 1907 (2000).
6. E. Diez, A. Sanchez, and F. Dominguez-Adame, Phys. Lett. A **12**, 1907 (2000).
7. D. Wittaut, S. Mossman, and H.J. Korsch, J. Phys. A **38**, 1777 (2005).
8. L.D. Carr, C.W. Clark, and W.P. Reinhardt, Phys. Rev. A **62**, 063610 (2000).
9. K. Rapedius, D. Wittaut, and H.J. Korsch, Phys. Rev. A **73**, 033608 (2006).
10. K. Rapedius and H.J. Korsch, J. Phys. A **42**, 425301 (2009).

11. V.P. Kraynov and H.A. Ishkhanyan, *Phys. Scr.* **40**, 014052 (2010).
12. V.F. Elesin, I.Yu. Kateev, and M.A. Remnev, *Semiconductors* **43**, 257 (2009).
13. V.F. Elesin, *JETP* **95**, 114 (2002).
14. N.V. Tkach and Yu.A. Seti, *Low Temp. Phys.* **35**, 556 (2009).
15. L.D. Landau and E.M. Lifshitz, *Quantum Mechanics. Non-Relativistic Theory* (Pergamon Press, New York, 1977).
16. J. Faist, F. Capasso, D.L. Sivco, C. Sirtori, A.L. Hutchinson, and A.Y. Cho, *Science* **264**, 553 (1994).
17. C. Gmachl, F. Capasso, D.L. Sivco, and A.Y. Cho, *Rep. Prog. Phys.* **64**, 1533 (2001).
18. L. Diehl, D. Bour, S. Corzine, J. Zhu, G. Hofler, M. Loncar, M. Troccoli, and F. Capasso, *Appl. Phys. Lett.* **88**, 201115 (2006).
19. Q.J. Wang, C. Pflug, L. Diehl, F. Capasso, T. Edamura, S. Furuta, M. Yamanishi, and H. Kan, *Appl. Phys. Lett.* **94**, 011103 (2009).

Received 26.08.11.

Translated from Ukrainian by O.I. Voitenko

ВПЛИВ НЕЛІНІЙНОЇ  
МІЖЕЛЕКТРОННОЇ ВЗАЄМОДІЇ  
НА ТУНЕЛЮВАННЯ ЕЛЕКТРОНІВ  
КРІЗЬ НЕСИМЕТРИЧНУ ДВОБАР'ЄРНУ  
РЕЗОНАНСНО-ТУНЕЛЬНУ СТРУКТУРУ

*М.В. Ткач, Ю.О. Сети, І.В. Бойко*

Резюме

У моделі ефективних мас і прямокутних потенціалів, враховуючи взаємодію між електронами, розвинуто квантово-механічну теорію коефіцієнта прозорості, позитивної і від'ємної провідностей моноенергетичного пучка електронів крізь відкриту плоску несиметричну двобар'єрну резонансно-тунельну структуру, яка може бути активним елементом квантового каскадного лазера чи квантового каскадного детектора. На прикладі несиметричної двобар'єрної резонансно-тунельної структури встановлено властивості коефіцієнта прозорості і провідності наносистеми залежно від енергії електронів та частоти електромагнітного поля. Показано, як властивості активної провідності можуть бути використані для експериментальної оцінки резонансних енергій та резонансних ширин електронних квазістаціонарних станів.